Mausam, (1995), **46**, 3, 235-244

551.557 : 551.513.1 : 551.553.21

Momentum budget of low level westerly jet during monsoon onset

P. S. JOSAN*

Cochin University of Science & Technology, School of Marine Sciences

(Received 16 March 1994, Modified 26 April 1994)

सार — मानसून के आरंभ के दिनों के दौरान निम्न स्तर पश्चिमी जेट के बनने और उसके वेग के बढ़ने/मंद होने के स्रोत तथा क्षीण होने की शैली का पता लगाने के लिए इस शोध पत्र में विश्लेषणात्मक अध्ययन किया गया है। इसके लिए संवेग बजट तकनीक का उपयोग किया गया है। बजट समीकरण को (x, y, p, t) पद्धति में प्राप्त किया गया है। अध्ययन के विषय का क्षेत्र एक छोटे बक्सानुमा आकार का है जिसकी सीमाएं मध्य अरब सागर तक हैं और उस क्षेत्र में मानसून के आरंभ के दिनों के दौरान पश्चिमी प्रवाह बहुत अधिक रहता है। बजट समीकरण में प्रत्येक पद की गणना अलग से की गई है। विश्लेषण के लिए एफ जी जी ई-III बी, 12 यू० टी० सी० आंकड़ा सेट का उपयोग किया गया। यह ज्ञात हुआ कि कोरिओलिस बल शैली, स्रोत शैली की अपेक्षा मंद शैली है। जब औसत समय संवेग बजट का विचार किया जाता है तो उत्तरी-दक्षिणी क्षणिक शैली मुख्य स्रोत शैली होती है। जब प्रत्येक दाब खंड के औसत समय संवेग बजट पर विचार किया जाता है तो यह निष्कर्ष निकलता है कि उत्तरी-दक्षिणी बल शैली सभी खंडों के संवेग की मुख्य स्रोत शैली है और बड़े कपासी प्रकार के संवहन से ऊपरी दाब खंडों हेतु संवेग का भिन्नात्मक क्षय हो सकता है। प्रत्येक दिन के संवेग बजट के परीक्षण से यह ज्ञात हुआ कि भिन्नात्मक बल, जेट के मंद होने की मुख्य शैली है और स्रोत शैली में प्रतिदिन परिवर्तन होता रहता है। मानसून के आने की अवधि के दौरान जेट में औसत रूप से वृद्धि होती है। यह भी ज्ञात हुआ कि प्रधार (जेट) की संवेग प्रवृत्ति कम होती है और उसकी प्रवृत्ति अस्थिर (दोलक) होती है। यह भी पता चला कि अल्प वर्षा, संवेग प्रवृत्ति से विलोमतः संबंधित है और जब भी जेट प्रबल अथवा क्षीण होता है तब वर्षा कम या अधिक होती है। U-संवेग के वितरण की प्रकृति को भी अस्थिर (दोलक) पाया गया।

ABSTRACT. In this paper a diagnostic study is carried out to find out the source and sink terms for the formation and acceleration/deceleration of low level westerly jet during monsoon onset. For this purpose momentum budget technique is used. The budget equation is derived in the (x, y, p, t) system. The area is confined to a small box with boundaries over the central Arabian Sea where the westerly flow is prominent during the onset of monsoon. Each term in the budget equation is calculated separately. FGGE III b. 1200 UTC data set is used for the analysis. The Coriolis force term is found to be sink term rather than a source term. Transient north-south term is prominent source term when time averaged momentum budget is considered. When the time averaged momentum budget for each pressure slab is considered, it is concluded that, north-south force terms are prominent source terms of momentum for all slabs and large cumulus type convection may contribute to frictional dissipation of momentum for the upper pressure slabs. Frictional force is the main sink term when one examines the momentum budget for each day and the source terms are varying day-by-day. On the average, the jet is accelerated during the period. It is also found that the net momentum tendency is small and oscillatory in nature. It is also found that at Minicoy, rainfall is inversely related to momentum tendency and whenever westerly jet is strong (weak) the rainfall is less (more). Distribution of U-momentum is also found to be oscillatory in nature.

Key words — Momentum, Convection, Zonal, Meridional, Westerly jet, Frictional force, Coriolis force.

1. Introduction

In this study, an effort is made to understand the evolution and maintenance of the low level westerly jet over the central Arabian Sea during the onset phase of southwest monsoon. For this purpose one can use the momentum budget technique. Each term in the budget equation is calculated quantitatively during the eight-day period covering the onset phase of 1979 monsoon, so that one can understand the large scale convergence and the role of cumulus convections in the vertical transport of momentum flux. The monsoon region is noted for the strongest westerly zonal flows in the lower troposphere of the tropical belt and closely coupled with deep convective activity. It is noted by many authors that the westerly wind bursts associated with this convection contribute to an increase of the angular momentum of the atmosphere and in turn slowing down the earth's rotation for the conservation of angular momentum.

Berson and Troup (1961), on the angular momentum balance in the equatorial trough zone of the eastern hemisphere, studied the conditions for seasonal balance of zonal angular momentum, during southern summer, in the troposphere overlying the equatorial (monsoonal) westerlies. It was shown that by and large the balance could be accounted for by zonal pressure gradients and meridional transport of earth's angular or Ω-momentum (a Coriolis effect).

Keshavamurthy (1968) studied the maintenance of the westerlies in the lower troposphere and the easterlies in the upper troposphere in the Indian

* Present affiliation : L. B. S. Centre for Science & Technology, Kunnamkulam, Kerala

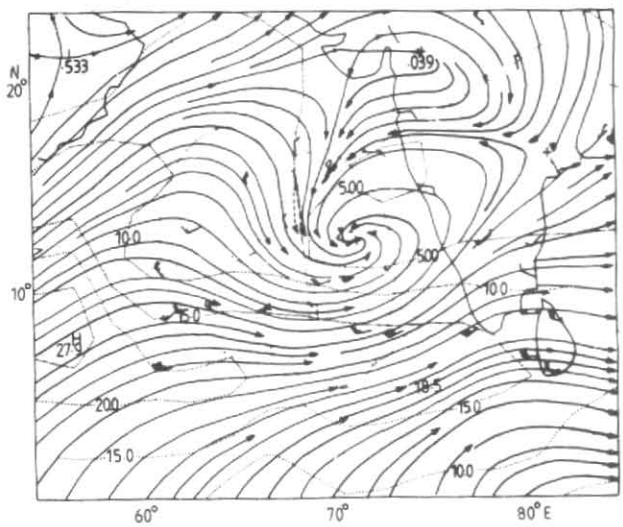

Fig. 1. The verification chart for the 850 hPa at 1200 UTC (June 15, 1979). The solid lines are isotachs (ms^{-1}). (After Krishnamurti, *et al.*, 1980)

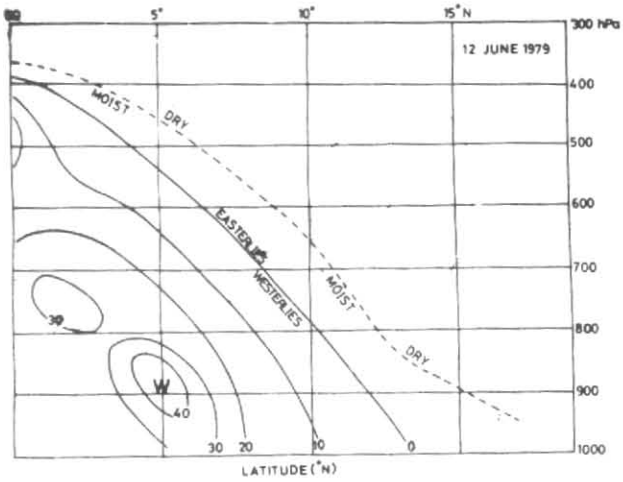

Fig. 2. Vertical cross-section through low-level westerly jet along 73° E from drop wind sondes of MONEX aircraft (NASA CV-990). (After Kuettner and Unninayar, 1980)

southwest monsoon by considering the angular momentum balance in the region. The main source term for the zonal angular momentum is found to be Coriolis or Ω-transport term. Schneinder and Lindzen (1976) showed that 'cumulus friction' is important in the momentum balance in the tropics and they parameterize the same. Holopainen *et al.* (1980) did a diagnostic study of the time-averaged budget of atmospheric zonal momentum over North America. The terms in the time mean zonal momentum equation, which depend only on the large scale motions, are evaluated for the region during the winter season. They found that zonal momentum is produced in the free atmosphere over North America by a local, thermally direct meridional circulation, with mean poleward ageostrophic flow above 700 hPa and the flux divergence associated with large scale vertical transports appears to be insignificant. Swinbank (1985) studied the global atmospheric angular momentum balance inferred from analysis made during the First GARP Global Experiment (FGGE). He found that the mountain torque is the main contributor to the short-term variation in the global atmospheric angular momentum. Krishnamurti *et al.* (1992) studied angular momentum, length of day and monsoonal low frequency mode. They studied some global aspects of intra-seasonal oscillations on the time scale of 30 to 50 days using length of the day as the point of reference. They tried to inter-connect the convection and transfer of momentum between earth and atmosphere and also the relation between length of day and angular momentum. They presented this cycle starting from a super cloud cluster at the near equatorial latitudes and this seems to be accompanied with an acceleration of zonal flows, an increase of atmospheric angular momentum and an increase in the length of day. The strongest low level westerly zonal flows were noted over the monsoon regions and they appear to be closely coupled to the deep convective activity. Over this region, a subsequent weakening of near equatorial zonal flows seems to be a response to the meridional motion of cloudy areas.

1.1. *Low level westerly jet*

The strengthening of the lower tropospheric westerlies in the Arabian Sea is an indication for increase of monsoon rains along the west coast of the Indian peninsula at the time of onset (Ananthakrishnan *et al.* 1968). Findlater's [1969 (a & b)] work has clearly established that southern hemispheric air of differing origin is organised and accelerated into a well defind stream which crosses the equator in a limited zone of longitude and becomes the southwest monsoon flow of the Arabian Sea. It is observed that during the entire period of southwest monsoon, a low level westerly jet of speed about 30 kt or more blows over the Arabian Sea with the core at about 850 hPa level. Joseph and Raman (1966) found, for the first time, that the low level westerly winds over peninsular India during July have a jet-like structure.

The monsoon onset vortex forms on this jet's barotropically unstable northern flank, and carries the monsoon farther north. Before MONEX-79 this jet was considered to be an arm split of Findlater jet,

which has its core near Somali coast. Extensive studies were carried out during the onset of 1979 monsoon in the MONEX programme. Many authors [Krishnamurti *et al.* (1980) and Gupta *et al.* (1980)] found that this jet had a strong core over western Arabian Sea between 8°-14°N latitudes at a level of 1.0 km and also had a separate identity.

Kuettner and Unninayar (1980), regarding the origin of this jet, suggest an inertial current steered by the cross equatorial pressure gradient and the northward movement of the jet axis should be correlated with increase in the pressure gradient. They, however, found no indication that the flow leading into this jet passed over Somali as indicated by Findlater (1971) although this might happen occasionally.

As mentioned in the earlier section, the monsoon onset took place with sudden change in the lower and upper tropospheric wind system. Of these the low level jet has a very significant role in the formation of onset vortex and the onset vortex causes the westerly jet to amplify. In Fig. 1 the westerly wind field is shown during the onset vortex formation. So, in order to diagnose the maintenance of westerly jet, the momentum budget is examined. One can find out each and every contributing term quantitatively and determine the source and sink terms, in the evolution of monsoon westerly jet.

1.2. *Period and area of study*

During MONEX-79, the onset of monsoon was on 14 June over Kerala. The low level westerly jet intensified during 10 to 17 June, with a maximum on 17 June. From Fig. 1 it is clearly seen that onset vortex has formed and the westerlies have intensified. After 17 June the vortex was found to be dissipating. So, the period chosen was 10-17 June (8 days). In order to include the spatial variation of the jet core during this period, one can choose the area between 0-20.625°N and 52.5°-78.75°E, since after hitting the southwest coast the strength of the jet drastically decreased. The south-westerly winds prevailed between 1000 to 500 hPa for the entire period with a core of strong winds at 850 hPa. So, 1000-500 hPa layer was chosen as the vertical extent of the region for computation and the data is available on the mesh with a width of 1.875°. Fig. 2 shows the vertical distribution of the westerlies between equator and 17°N, which shows that jet core is situated around 850 hPa.

1.3. *Momentum budget equation*

Since the area considered is small and near to the equator, the effect due to curvature of the earth's surface can be neglected and so one can choose safely the cartesian coordinate (x, y, p, t) system. By combining and integrating the zonal component of momentum equation and the equation of continuity in isobaric coordinate system for the horizontal boundaries x_1 to x_2, y_1 to y_2 and to the pressure levels p_1 to p_2 one can obtain the momentum budget equation per unit mass as follows :

$$\frac{1}{|\overline{M}|}\frac{1}{g}\int_{x_1}^{x_2}\int_{y_1}^{y_2}\int_{p_1}^{p_2}\frac{\partial \bar{u}}{\partial t}\,dx\,dy\,dp = 0$$

$$= \frac{1}{|\overline{M}|}\left[\frac{-1}{g}\int_{y_1}^{y_2}\int_{p_1}^{p_2}(\bar{u}^2)_{x_1}^{x_2}\,dp\,dy\right.$$

(A)

$$-\frac{1}{g}\int_{y_1}^{y_2}\int_{p_1}^{p_2}(\bar{u}'^2)_{x_1}^{x_2}\,dp\,dy$$

(B)

$$-\frac{1}{g}\int_{x_1}^{x_2}\int_{p_1}^{p_2}(\bar{u}\bar{v})_{y_1}^{y_2}\,dp\,dx$$

(C)

$$-\frac{1}{g}\int_{x_1}^{x_2}\int_{p_1}^{p_2}(\overline{u'v'})_{y_1}^{y_2}\,dp\,dx$$

(D)

$$-\frac{1}{g}\int_{x_1}^{x_2}\int_{y_1}^{y_2}(\bar{u}\bar{w})_{p_1}^{p_2}\,dx\,dy$$

(E)

$$-\frac{1}{g}\int_{x_1}^{x_2}\int_{y_1}^{y_2}(\overline{u'w'})_{p_1}^{p_2}\,dx\,dy$$

(F)

$$+\frac{2\Omega}{g}\int_{x_1}^{x_2}\int_{y_1}^{y_2}\int_{p_1}^{p_2}\bar{V}\,\mathrm{Sin}\,\phi\,dx\,dy\,dp$$

(G)

$$-\int_{y_1}^{y_2}\int_{p_1}^{p_2}(\bar{Z})_{x_1}^{x_2}\,dy\,dp$$

(H)

$$\left.+\int_{x_1}^{x_2}\int_{y_1}^{y_2}(\bar{\tau}_{zx})_{p_1}\,dy\,dx\right] \qquad (1)$$

(I)

(See Appendix for derivation)

TABLE 1

The average momentum budget per unit mass between 1000-500 hPa in vertical, equator to 20.625°N in meridional and 52.5°E to 78.75°E in the zonal direction in units of M sec^{-2} for the period 10-17 June 1979

S. No.	Description	Term	Magnitude (M sec^{-2})
1.	Coriolis force term	T_1	$-.733 \times 10^{-3}$
2.	Frictional force term (for 1000 hPa)	T_2	$-.605 \times 10^{-2}$
3.	Zonal pressure gradient term	T_3	$.564 \times 10^{-2}$
4.	Mean east-west term	T_4	$.306 \times 10^{-2}$
5.	Transient east-west term	T_5	$.298 \times 10^{-2}$
6.	Mean north-south term	T_6	$.762 \times 10^{-2}$
7.	Transient north-south term	T_7	$.668 \times 10^{-1}$
8.	Mean top-bottom term	T_8	$.351 \times 10^{-9}$
9.	Transient top-bottom term	T_9	$-.186 \times 10^{-8}$
		Total	.07931

And also take time-average of the perturbed quantities. The upper level friction and mountain force are neglected. In the above Eqn. (1),

C_D — The average non-dimensional drag coefficient

g — acceleration due to gravity

Ω — angular velocity of the earth

$M = \dfrac{(x_2-x_1)\ (y_2-y_1)\ (p_2-p_1)}{g}$ = entire mass of the box

p_1 — lower level

p_2 — upper level

ρ — density of the air

u — zonal component of wind

v — meridional component of wind

V — horizontal velocity

w — vertical pressure velocity

x_1 — western boundary

x_2 — eastern boundary

y_1 — southern boundary

y_2 — northern boundary

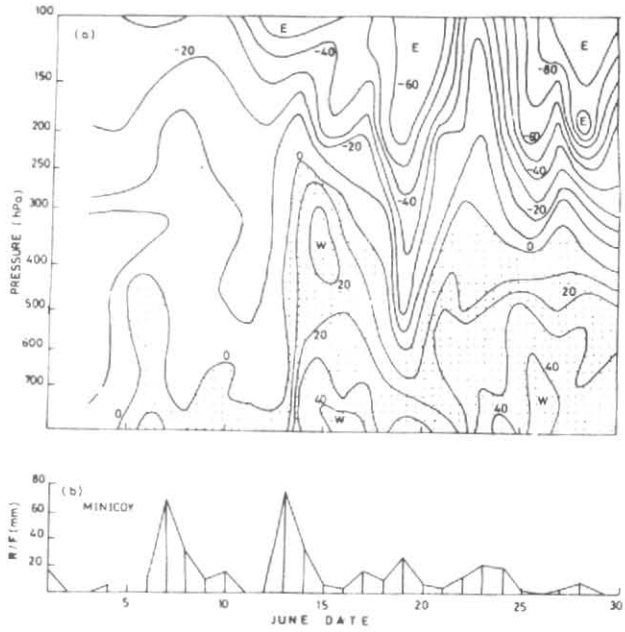

Figs. 3 (a & b). (a) Vertical time-section of zonal wind (upper) isopleth in knots (Dotted area-westerlies) and (b) Rainfall pattern (lower) for station Minicoy. (After Shrestha 1980)

z — Geopotential height

$\tau_{zx} = C_D \rho_u (u^2 + v^2)^{1/2}$

— The eddy stress due to the zonal motion

The value for C_D over ocean,

$C_D = C_{D_0}\ (0.74 + 0.046\ V)$ for V $5.8 < V < 16.8$ ms^{-1}

are used where $C_{D_0} = 1.1 \times 10^{-3}$ (after Krishnamurti 1980). Other symbols have usual meaning. The bar denotes time averaging and the dashes denote deviation from this time-mean.

The right hand side of the balance equation represents the various forces acting in the box. Term (A) is the east-west term due to the mean zonal flow between the boundaries and term (B) is the transient east-west term due to perturbation movements in the east-west boundaries. The terms (C) and (D) are the mean and transient north-south terms due to mean and perturbed north-south flows between north-south boundaries. (E) and (F) are the mean and transient top-bottom terms due to mean and perturbed top-bottom flows between the boundaries. (G) is the Coriolis force term due to the Coriolis turning due to the rotation of earth when air is moving in meridional direction. (H) is the zonal pressure gradient force term due to zonal mean

TABLE 2

Time-averaged momentum per unit mass for each pressure slab in units of M sec^{-2}

Slab	T_1	T_2	T_3	T_4	T_5	T_6	T_7	T_8	T_9	Total
1000 — 850 hPa	−.0041	−.0202	.0126	.0118	.011	.523	1.11	−.00918	.00512	1.64
850 — 700 hPa	−.0036	?	.0168	.00547	.0081	8.01	94.9	.00143	.0261	103
700 — 500 hPa	−.00389	?	.0046	.00219	.0009	12.7	95.1	.00582	−.0234	108

geopotential height gradient. (I) is the frictional force, surface skin friction due to zonal motion.

During the period and for the region considered, the zonal wind is westerly. So the momentum would be given to the earth from the atmosphere. The zonal pressure gradient is considered to be large. Since in the beginning of the period, *i.e.*, before onset, the zonal circulation is prominent and after the onset the meridional circulation is predominant. So, it can be expected that the east-west terms will be larger than the north-south terms in the beginning of the period and *vice-versa* after the onset. As found in the previous studies by Berson and Troup (1961) and Keshavamurthy (1968), the contribution from the Coriolis force term is also expected to be quite significant. Again, top-bottom terms (both mean and transient) are expected to reveal significant points regarding the cumulus convection and zonal flow acceleration during the period. In Fig. 3 one can see that the rainfall maxima is associated with the westerly wind minima and *vice-versa*. So, from this observed interrelation one can understand about the interaction between the convection and zonal westerly flow acceleration/deceleration.

2. Data and method

The re-analysed Global FGGE level III-b data set is used which was prepared by European Centre for Medium Range and Weather Forecasts. The parameters used are u and v components of wind and geopotential height for the levels of 1000, 850, 700and 500 hPa of 1200 UTC data set. The terms in the balance equation are computed separately. The evaluation of integrals are performed numerically by using Tropezoidal rule. Vertical velocity w (x, y, p, t) is calculated by kinematic method from u and v data.

3. Results and discussion

There are mainly three results.

3.1. *Time-averaged momentum budget for the box*

The nine terms computed are depicted in Table 1. The maximum contribution is found to be due to transient north-south term (T_7). The Coriolis term (T_2) is found to be less and destroying the momentum from the box. Top-bottom terms (T_8, T_9) are very small compared to other terms. The terms destroy the momentum are transient top-bottom, Coriolis, and frictional force terms and the last term is found to be the largest. The other six terms are the source terms contributing the momentum to the box as given in the table.

3.2. *Time-averaged momentum budget per unit mass for each pressure-slab*

In Table 2 the budgets are given for all the three slabs. For all the slabs, the contributing terms for the momentum are zonal pressure gradient force term (T_3), east-west terms (T_4, T_5) and north-south terms (T_6, T_7). Among these, north-south force terms are several orders higher than the others. The sink terms destroying the momentum are Coriolis and frictional force terms (T_1, T_2). The mean top-bottom term (T_8) is a sink term in the slab 1000-850 hPa, while it is a source term for the other two slabs. The transient top-bottom term (T_9) is source term for the 1000-850 hPa and 850-700 hPa slabs while it is a sink term for the 700-500 hPa slab. Total residual momentum shoots up from 1.64 units in the lower slab to 103 units in the 850-700 hPa slab. This excess should be transported by some other mechanism, so that no residual momentum is left, since the surface frictional effect will be very small at this level, the cumulus friction can be taken into account.

3.3. *The momentum budget for each day*

This budget is without time averaging. The term in the budget equation are Coriolis force (T_1), frictional force (T_2), zonal pressure gradient (T_3), east-west (T_4), north-south (T_5) and top-bottom (T_6) terms. The budget from 10 to

TABLE 3

Momentum budget per unit mass between 1000-500 hPa, equator to 20.625°N and 52.5°E to 78.75°E in units of M sec^{-2} for eight days of June 1979

Day	T_1	T_2	T_3	T_4	T_5	T_6	Total
10th	−.00049	−.014	.0118	−.00372	.00016	$.725\times10^{-11}$	−0.0062
11th	−.00007	−.00589	.0144	.00131	−.0004	$.215\times10^{-9}$	.0093
12th	−.00049	−.0216	−.00268	−.00961	.00755	$.563\times10^{-9}$	−.0268
13th	−.00072	−.00994	−.00268	.0245	.013	$-.796\times10^{-9}$	.0242
14th	−.00062	−.164	.00591	.0257	.0177	$-.376\times10^{-8}$	−.115
15th	−.00084	−.187	.0177	.00023	.0183	$-.287\times10^{-8}$	−.151
16th	−.000951	−.0512	−.00658	.00081	.0236	$-.338\times10^{-8}$	−.0343
17th	−.00238	.189	.015	.00253	1.02	$-.177\times10^{-7}$	0.846

17 June is presented in Table 3. The Coriolis force term is found to be a few orders less than the other terms. The top-bottom term is the least contributing term. In general, frictional force term is the main dissipation term for momentum throughout the period. The main contributing term varies each day. But one can say that the frictional force, zonal pressure gradient, east-west and north-south terms are predominant in the daily budgets. The jet is having relatively high deceleration during the first day as indicated by the total sum of all terms in the Table 3. The next day, the jet is slightly accelerated and then decelerated. And on 12 June there is acceleration. During the next three days, the jet is decelerated substantially. And a very high acceleration of the jet occurs on 17th. In Fig. 4 plot of time (days) *versus* net rate of change of momentum per unit mass per sec is depicted. One can observe that the net momentum tendency is small and oscillating around zero value until 17th when sudden increase in net momentum tendency is observed and the north-south term (T_5) is the largest contributor.

3.4. *Distribution of U-momentum*

In Fig. 5 the U-momentum distribution is depicted graphically for each day. It is oscillatory in nature.

U-momentum for the box is given by,

$$\frac{\frac{1}{g}\int_{x_1}^{x_2}\int_{y_1}^{y_2}\int_{p_1}^{p_2} u\,dx\,dy\,dp}{\left|\frac{(x_2-x_1)(y_2-y_1)(p_2-p_1)}{g}\right|}$$

U-momentum is maximum on 14 and 17 June for the whole box. A comparison between Figs. 4 and 5 shows that the two peaks in U-momentum on 14 and 15 are caused by the positive and negative momentum tendency spells (Fig. 4) observed on 13 and 14/15 June respectively. The lag of about one-day between the two sets of peaks is observed.

4. Conclusions

(*i*) The time-averaged momentum budget for the box considered suggests that; (a) The maximum contribution for the maintenance of westerly jet is due to transient north-south term and (b) the Coriolis force term is found to be less and emerges as a sink term for the momentum alongwith transient top-bottom and frictional force terms.

(*ii*) Time-averaged momentum budget per unit mass for each pressure slab suggests that in all the three slabs the north-south forcing (T_6 & T_7) terms are several orders larger than the other terms in magnitude and they are source terms for the momentum. The Coriolis and frictional force terms are the major sink terms. And from Table 2, one can observe that, the total residual momentum shoots up from 1000-850 hPa slab to 850-700 hPa slab. This may be explained by including the cumulus friction force into the budget.

(*iii*) Regarding the momentum budget for each day frictional force is the main sink term and there are no fixed source terms since they vary day-by-day. But one can identify frictional force, zonal pressure gradient force and east-west and north-south

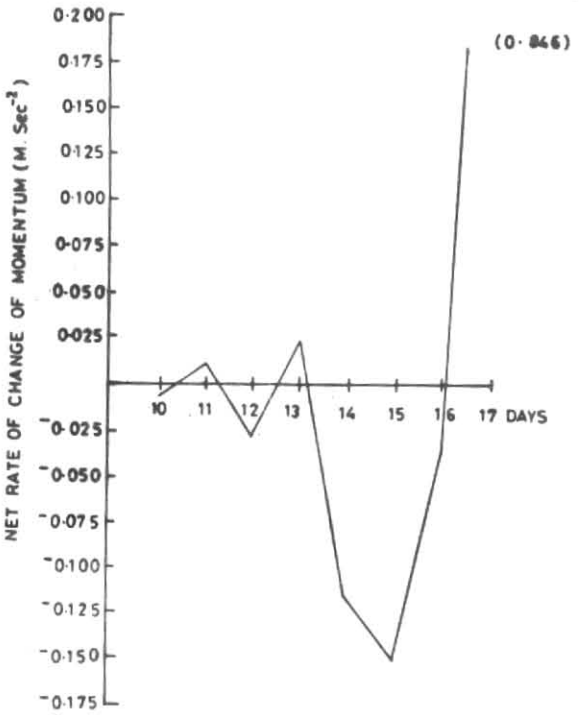

Fig. 4. Plot of time (days) *versus* net rate of change of momentum per unit mass per sec

terms are predominant in the daily budgets. Only spectacular increase is due to north-south term on 16-17 June, which is revealed in the daily budget. This is in association with the dramatic increase of U-momentum at the same time. The increase on 13-14 June during the formation of the vortex and then the decrease within 24 hours can be examined clearly from an energy budget. The net momentum tendency is small and oscillating around zero value until 17 June. The jet is accelerated and decelerated during the period in an oscillatory nature. On the final day there is very high acceleration and on the average the jet is accelerated.

By examining Figs. 3 & 4 together, one can observe that the rainfall at Minicoy and the momentum tendency have inverse relationship between them and whenever westerly jet is strong (weak) the rainfall is less (more). This shows the importance of cumulus friction in the momentum budget of the westerly jet. Distribution of U-momentum is also oscillatory in nature when depicted on a graph. In future, friction can be parameterized more accurately. It is possible to introduce cumulus friction, since for the tropical region it is very important. Mountain effect and gravity wave drag may also be included for lower levels, as they may have important role in shaping up the monsoon westerly jet. The inability to include above-said processes may lead to error

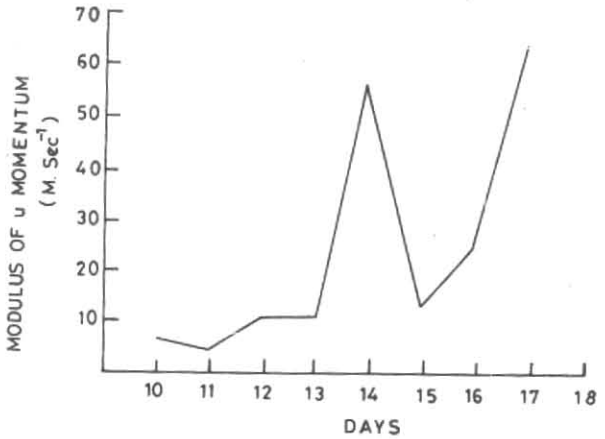

Fig. 5. Distribution of U-momentum

amplification in some of the results and the external forces acting on the boundaries are also neglected.

Acknowledgements

The author wishes to express his deep gratitude to Dr. S. K. Mishra, Director, National Centre for Medium Range Weather Forecasting (NCMRWF), New Delhi, for his valuable suggestions and proper guidance during the period of this work. The author wishes to thank Director, Indian Institute of Tropical Meteorology, Pune for giving him all the facilities necessary for this work. He also wishes to express his sincere thanks to Prof. H. S. Ram Mohan, Co-ordinator, M. Tech. Atmospheric Sciences Programme, Physical Oceanography and Meteorology Division, School of Marine Sciences, Cochin University of Science and Technology, for all the encouraging attitudes from his side during this work.

APPENDIX

Since the area considered is small and near to the equator, the effect due to curvature of the earth's surface can be neglected and so one can choose safely the cartesian coordinate system.

The absolute momentum of the earth-atmosphere closed system is the sum of momentum due to the rotation of earth and momentum due to the relative motion of the air parcel with respect to the earth. It should be constant according to law of conservation of linear momentum. The absolute momentum of an air parcel of unit mass can be written as

$$p = \Omega a \cos\phi + u \qquad (3.1)$$

where Ω — angular speed of rotation of the earth, a — mean radius of the earth; u — relative zonal wind speed and ϕ any arbitrary latitude.

From Newton's Second Law of motion, changes in linear momentum of the parcel can come through the action of forces acting on it, *i.e.*,

$$\frac{dp}{dt} = \frac{-\partial\phi}{\partial x} + Fx \qquad (3.2)$$

That is, the sum of east-west pressure gradient force per unit mass and the frictional force per unit mass against the flow; since we are considering only the zonal motion. The zonal component of momentum equation in isobaric coordinate system is given by,

$$\frac{\partial u}{\partial t} + u\frac{\partial u}{\partial x} + v\frac{\partial u}{\partial y} + w\frac{\partial u}{\partial p} - 2\Omega v \sin\phi = \frac{-\partial\phi}{\partial x} + Fx \qquad (3.3)$$

after neglecting the term involving w.

The equation of continuity in the system is given by

$$\frac{\partial u}{\partial x} + \frac{\partial v}{\partial y} + \frac{\partial w}{\partial p} = 0 \qquad (3.4)$$

One can combine both the above equations as follows :

$$\frac{\partial u}{\partial t} + \frac{\partial(u^2)}{\partial x} + \frac{\partial(uv)}{\partial y} + \frac{\partial(wu)}{\partial p} - 2\Omega v \sin\phi = \frac{-\partial\phi}{\partial x} + Fx \qquad (3.5)$$

$$= \frac{dp}{dt} \quad \text{as per (3.2)}$$

The above equation represents the rate of change of absolute momentum per unit mass. Then, if we consider an element of mass $dm = \left(\frac{-dx\,dy\,dp}{g}\right)$ and by multiplying Eqn. (3.5) and rearranging the terms and integrating for the regions x_1 to x_2, y_1 to y_2 and p_1 to p_2, one can obtain.

$$\frac{1}{g}\int_{x_1}^{x_2}\int_{y_1}^{y_2}\int_{p_1}^{p_2}\frac{\partial u}{\partial t}\,dx\,dy\,dp$$

$$= \frac{-1}{g}\int_{x_1}^{x_2}\int_{y_1}^{y_2}\int_{p_1}^{p_2}\frac{\partial}{\partial x}(u^2)\,dx\,dy\,dp$$

$$\frac{-1}{g}\int_{x_1}^{x_2}\int_{y_1}^{y_2}\int_{p_1}^{p_2}\frac{\partial}{\partial y}(uv)\,dx\,dy\,dp$$

$$\frac{-1}{g}\int_{x_1}^{x_2}\int_{y_1}^{y_2}\int_{p_1}^{p_2}\frac{\partial}{\partial p}(uw)\,dx\,dy\,dp$$

$$+ \frac{2\Omega}{g}\int_{x_1}^{x_2}\int_{y_1}^{y_2}\int_{p_1}^{p_2} v\sin\phi\,dx\,dy\,dp$$

$$- \frac{1}{g}\int_{x_1}^{x_2}\int_{y_1}^{y_2}\int_{p_1}^{p_2}\frac{\partial\phi}{\partial x}\,dx\,dy\,dp$$

$$+ \frac{1}{g}\int_{x_1}^{x_2}\int_{y_1}^{y_2}\int_{p_1}^{p_2} Fx\,dx\,dy\,dp \qquad (3.6)$$

After integrating the similar derivatives one can obtain.

$$\frac{1}{g}\int_{x_1}^{x_2}\int_{y_1}^{y_2}\int_{p_1}^{p_2}\frac{\partial u}{\partial t}\,dx\,dy\,dp$$

$$= \frac{-1}{g}\int_{y_1}^{y_2}\int_{p_1}^{p_2}(u^2)_{x_1}^{x_2}\,dp\,dy$$

$$- \frac{1}{g}\int_{x_1}^{x_2}\int_{p_1}^{p_2}(uv)_{y_1}^{y_2}\,dx\,dp$$

$$- \frac{1}{g}\int_{x_1}^{x_2}\int_{y_1}^{y_2}(uw)_{p_1}^{p_2}\,dx\,dy$$

$$+ \frac{2\Omega}{g}\int_{x_1}^{x_2}\int_{y_1}^{y_2}\int_{p_1}^{p_2} v\sin\phi\,dx\,dy\,dp$$

$$- \frac{1}{g}\int_{y_1}^{y_2}\int_{p_1}^{p_2}(\phi)_{x_1}^{x_2}\,dy\,dp$$

$$- \int_{x_1}^{x_2}\int_{y_1}^{y_2}(\tau_{zx})_{p_1}^{p_2}\,dy\,dx \qquad (3.7)$$

after putting $F_x = -g \dfrac{\partial \tau_{zx}}{\partial p}$. frictional force/unit mass and $\tau_{zx} = C_D \rho u V$ is the eddy stress due to the zonal motion: $V = (u^2 + v^2)^{1/2}$ is the horizontal velocity. By hydrostatic assumption $dp = -g\rho dz$ where, g is the acceleration due to gravity, ρ is the density of the air, C_D is the average non-dimensional drag coefficient. The accepted values for C_D over ocean are

$$C_D = C_{D_0} = 1.1 \times 10^{-3} \qquad \text{for } V < 5.8 \text{ ms}^{-1}$$

$$= C_{D_0}(0.74 + 0.046\, V) \qquad \text{for } 5.8 < V < 16.8 \text{ ms}^{-1}$$

$$= C_{D_0}(0.94 + 0.034\, V) \qquad \text{for } V > 16.8 \text{ ms}^{-1}$$

(after Krishnamurti 1980)

Again, if we divide the whole equation by the entire mass of the box $|M| = \left|\dfrac{(x_2-x_1)(y_2-y_1)(p_2-p_1)}{g}\right|$

one can obtain the equation as

$$\frac{1}{|M|}\frac{1}{g}\int_{x_1}^{x_2}\int_{y_1}^{y_2}\int_{p_1}^{p_2}\frac{\partial u}{\partial t}\,dx\,dy\,dp$$

$$= \frac{1}{|M|}\left[\frac{-1}{g}\int_{y_1}^{y_2}\int_{p_1}^{p_2}(u^2)_{x_1}^{x_2}\,dy\,dp\right.$$

$$-\frac{1}{g}\int_{x_1}^{x_2}\int_{p_1}^{p_2}(u\,v)_{y_1}^{y_2}\,dx\,dp$$

$$-\frac{1}{g}\int_{x_1}^{x_2}\int_{y_1}^{y_2}(u\,w)_{p_1}^{p_2}\,dx\,dy$$

$$+\frac{2\Omega}{g}\int_{x_1}^{x_2}\int_{y_1}^{y_2}\int_{p_1}^{p_2} v\sin\phi\,dx\,dy\,dp$$

$$-\int_{y_1}^{y_2}\int_{p_1}^{p_2}(z)_{x_1}^{x_2}\,dy\,dp$$

$$\left.+\int_{x_1}^{x_2}\int_{y_1}^{y_2}(\tau_{zx})_{p_1}\,dy\,dx\right] \qquad (3.8)$$

by substituting for ϕ geopotential in the sixth term as gz and in the seventh term $(\tau_{zx})_{p_2} - (\tau_{zx})_{p_1} \simeq -(\tau_{zx})_{p_1}$. Since we are neglecting the upper level friction. The Eqn. (3.8) calculates the momentum per unit mass due to the total motion. Again, to calculate the individual contribution of standing motion and transient motion, we have to apply perturbation analysis. That is, $u = \bar{u} + u'$, $v = \bar{v} + v'$, $w = \bar{w} + w'$, $z = \bar{z} + z'$ etc.

$$\text{where, } \bar{u} = \frac{1}{t_2 - t_1}\int_{t_1}^{t_2} u\,dt \quad \text{etc.}$$

are the standing motion and the primed are the transient motion.

Substituting in the above equation one can obtain,

$$\frac{1}{|M|}\frac{1}{g}\int_{x_1}^{x_2}\int_{y_1}^{y_2}\int_{p_1}^{p_2}\frac{\partial}{\partial t}(\bar{u}+u')\,dx\,dy\,dp$$

$$= \frac{1}{|M|}\left[\frac{-1}{g}\int_{y_1}^{y_2}\int_{p_1}^{p_2}(\bar{u}^2+2\bar{u}u'+u'^2)_{x_1}^{x_2}\,dp\,dy\right.$$

$$-\frac{1}{g}\int_{x_1}^{x_2}\int_{p_1}^{p_2}(\bar{u}\bar{v}+u'v'+u'\bar{v}+v'\bar{u})_{y_1}^{y_2}\,dx\,dp$$

$$-\frac{1}{g}\int_{x_1}^{x_2}\int_{y_1}^{y_2}(\bar{u}\bar{w}+u'w'+\bar{u}w'+\bar{w}u')_{p_1}^{p_2}\,dx\,dy$$

$$+\frac{2\Omega}{g}\int_{x_1}^{x_2}\int_{y_1}^{y_2}\int_{p_1}^{p_2}(\bar{v}+v')\sin\phi\,dx\,dy\,dp$$

$$-\frac{1}{g}\int_{y_1}^{y_2}\int_{p_1}^{p_2}(\bar{z}+z')\,dy\,dp$$

$$\left.-\int_{x_1}^{x_2}\int_{y_1}^{y_2}(\bar{\tau}_{zx}+\tau'_{zx})_{p_1}\,dy\,dx\right] \qquad (3.9)$$

In the above equation in term-5 on right hand side, $(\bar{z})_{x_1}^{x_2}$ represents the zonal mean geopotential height gradient and $(z')_{x_1}^{x_2}$ is due to mountain. Since the geopotential height at the eastern and western sides of the mountains may not be equal, a force will be acting if mountain or sloped terrains are present. Again averaging with respect to time, the perturbations like $\bar{u}'$, $\bar{v}'$, $\bar{\tau}'_{zx}$, $\bar{u}v'$ and $\bar{u}\bar{w}'$ will vanish and the mountain force term can be neglected for the

region considered. So the final equation can be written as,

$$\frac{1}{|M|}\frac{1}{g}\int_{x_1}^{x_2}\int_{y_1}^{y_2}\int_{p_1}^{p_2}\frac{\partial \bar{u}}{\partial t}\,dx\,dy\,dp = 0$$

$$= \frac{1}{|M|}\left[\frac{-1}{g}\int_{y_1}^{y_2}\int_{p_1}^{p_2}(\bar{u}^2)\Big|_{x_1}^{x_2}\,dp\,dy\right.$$

$$-\frac{1}{g}\int_{y_1}^{y_2}\int_{p_1}^{p_2}(\bar{u}'^2)\Big|_{x_1}^{x_2}\,dp\,dy$$

$$-\frac{1}{g}\int_{x_1}^{x_2}\int_{p_1}^{p_2}(\bar{u}\,\bar{v})\Big|_{y_1}^{y_2}\,dp\,dx$$

$$-\frac{1}{g}\int_{x_1}^{x_2}\int_{p_1}^{p_2}(\overline{u'v'})\Big|_{y_1}^{y_2}\,dp\,dx$$

$$-\frac{1}{g}\int_{x_1}^{x_2}\int_{y_1}^{y_2}(\bar{u}\,\bar{w})\Big|_{p_1}^{p_2}\,dx\,dy$$

$$-\frac{1}{g}\int_{x_1}^{x_2}\int_{y_1}^{y_2}(\overline{u'w'})\Big|_{p_1}^{p_2}\,dx\,dy$$

$$+\frac{2\Omega}{g}\int_{x_1}^{x_2}\int_{y_1}^{y_2}\int_{p_1}^{p_2} v\sin\phi\,dx\,dy\,dp$$

$$-\int_{y_1}^{y_2}\int_{p_1}^{p_2}(\bar{z})\Big|_{x_1}^{x_2}\,dy\,dp$$

$$\left.+\int_{x_1}^{x_2}\int_{y_1}^{y_2}(\bar{\tau}_{zx})_{p_1}\,dy\,dx\right] \qquad (3.10)$$

References

Ananthakrishnan, R., *et al.*, 1968, FMU Report No. IV-18.2, India Meteorological Department Publication.

Berson, F. A. and Troup, A. J., 1961, "On the angular momentum balance in the equatorial trough zone of eastern hemisphere", *Tellus*, **XIII**, pp. 66-77.

Findlater, 1969 (a), "A major low level air current over the Indian Ocean during the northern summer", *Quart. J. R. Met. Soc.*, **95**, pp. 400-403.

Findlater, 1969 (b), "Interhemispheric transport of air into lower troposphere over the western Indian Ocean", *Quart. J. R. Met. Soc.*, **95**, pp. 362-380.

Findlater, 1971, "Mean monthly air flow at low levels over the western Indian Ocean", Geophys. Memo. No. 115, HMSO, London, U.K.

Gupta, M. G., Pant, M. C., Rawat, M. S. and Goel, I. C., 1980, "Low level jet stream over Arabian Sea during onset phase of monsoon 1979", FGGE Operations Report, **9**, pp. 275-290.

Holopainen, E. O., Lau, N. C. and Oort, A. H., 1980, "A diagnostic study of the time averaged budget of atmospheric zonal momentum over North America", *J. Atmos. Sci.*, 2234.

Joseph, P. V. and Raman, P. L., 1966, "Existence of low level westerly jet stream over peninsular India during July", *Indian J. Met. Hydrol. & Geophys.*, **17**, pp. 407-410.

Keshavamurthy, R. N., 1968, "On the maintenance of mean zonal motion in the Indian summer monsoon", *Mon. Weath. Rev.*, **96**, 1, pp. 23-31.

Krishnamurti, T. N., 1980, Work-book on Numerical Weather Prediction, WMO Publication, No. 669, pp. 1-2.

Krishnamurti, T. N., Ardanuy, P., Ramanathan, Y. and Pasch, R., 1980, "On the onset vortex of the summer monsoons, 9, Part B, FGGE Operations Report, pp. 115-166.

Krishnamurti, T. N., Sinha, M. C., Krishnamurti, Ruby, Oosternof, D. and Comeaux, J., 1992, "Angular momentum, length of day and monsoonal low frequency mode", *J. Met. Soc. of Japan*, **70**, 1, pp. 131-165.

Kuettner, J. P. and Unninayar, M.S., 1980, "The near equatorial jet south of India and its role in the onset of the monsoon", FGGE Operations Report, **9**, pp. 96-114.

Schneinder, E. K. and Lindzen, R. S., 1976, "A discussion of the parameterization of momentum exchange by cumulus convection", *J. Geophy. Res.*, **81**, pp. 3158-3160.

Shrestha, M. L., 1980, "Some aspects of the zonal wind profile during the onset of monsoon", GARP : FGGE Operation Report, **9**, Part A, pp. 7-15.

Swinbank, R., 1985, "The global atmosheric angular momentum balance inferred from analysis made during the FGGE", *Quart. J. R. Met. Soc.*, III, pp. 977-992.